Supporting information

The selective oxidation of methanol to formaldehyde using novel iron molybdate catalysts prepared by supercritical antisolvent precipitation

Jack R. Pitchers,[a*] James Carter,[a] Aziz Genç,[a] Thomas J.A. Slater,[a] David J. Morgan,[a] Alice Oakley,[b] Bart D. Vandegehuchte,[c] Stuart H. Taylor,[a] Graham J. Hutchings[a*]

a. J. R. Pitchers, J. Carter, A. Genç, T.J.A. Slater, D. Morgan, S. Taylor, G. Hutchings
Cardiff Catalysis Institute, School of Chemistry
Cardiff University
Translational Research Hub, Maindy Road Cardiff, UK

E-mail: pitchersjr@cardiff.ac.uk; hutch@cardiff.ac.uk Address here.

b. A. Oakley
School of Chemistry
Southampton University
Highfield Campus, Southampton, Hampshire, UK

c. B. D. Vandegehuchte
TotalEnergies OneTech Belgium
Zone Industrielle C, 7181 Feluy, Belgium

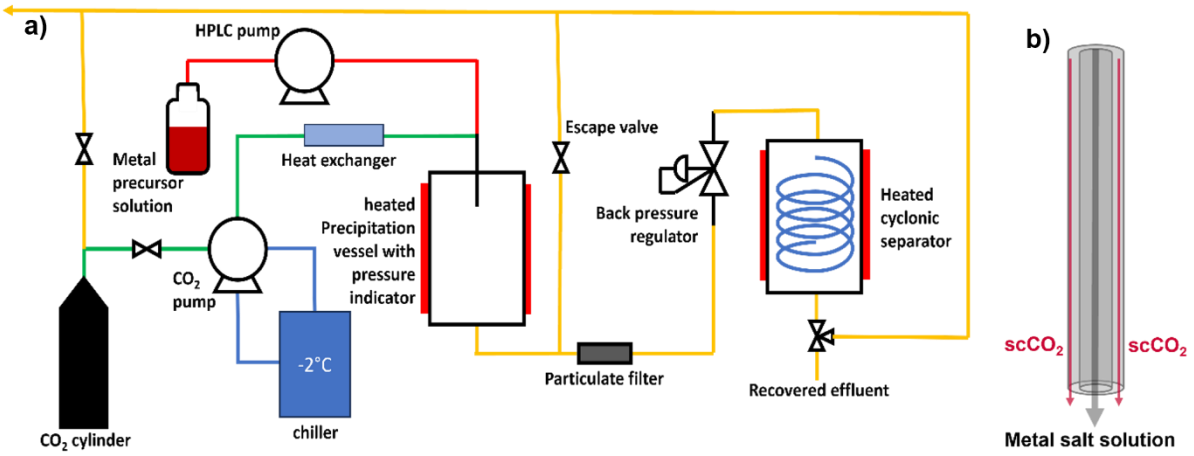

Fig S1. a) Schematic of Sci-Med custom apparatus for supercritical antisolvent precipitation with flow indications for CO_2 (green), coolant (blue), metal precursor solution (red) and ventilation (yellow). **b)** Coaxial nozzle design, highlighting the feed of CO_2 and metal precursor solution into the precipitation vessel.

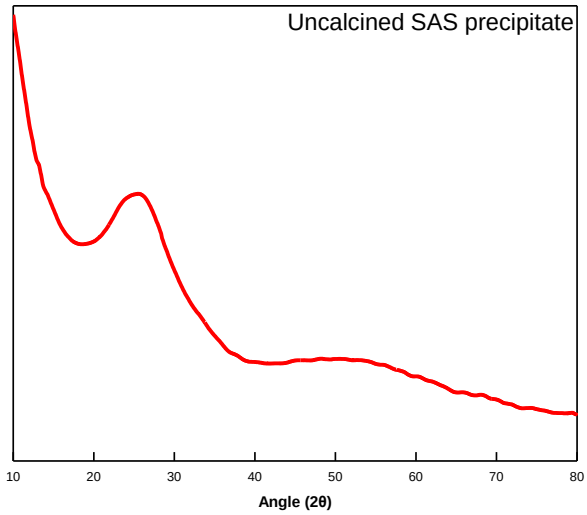

Fig S2. XRD diffractogram of a FeMo SAS precipitate, showing no well-defined crystalline structure.

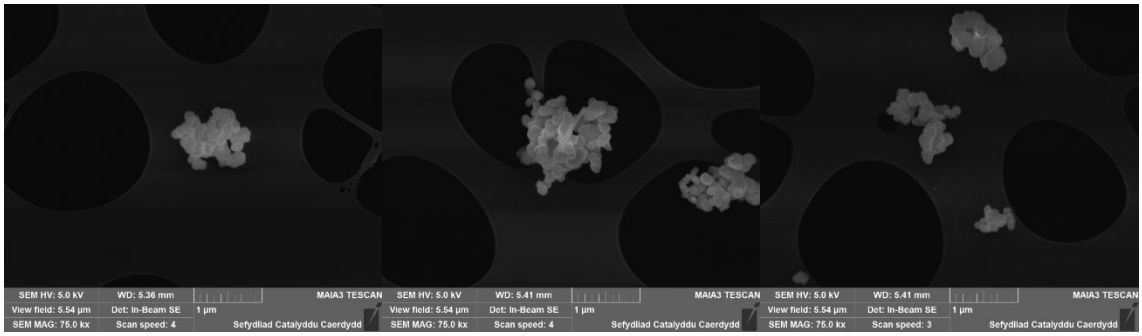

Fig S3. SEM images of FeMo_140P-10C-20W-7.5F.

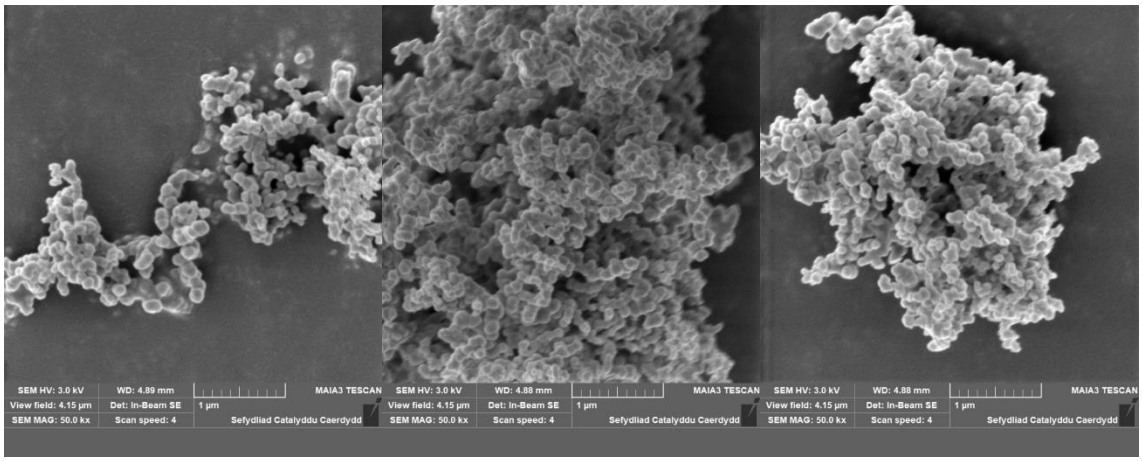

Fig S4. SEM images of FeMo_110P-5C-20W-5F.

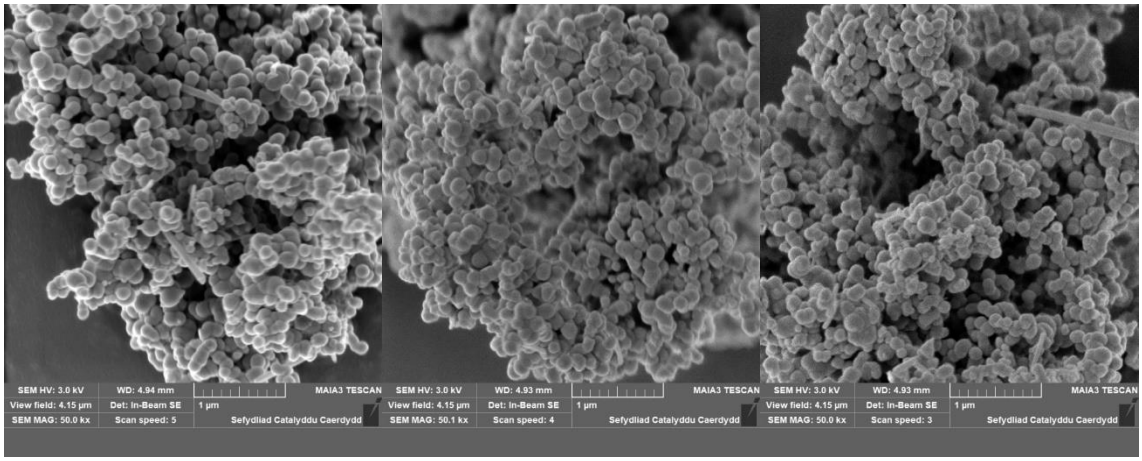

Fig S5. SEM images of FeMo_140P-10C-10.5W-5F.

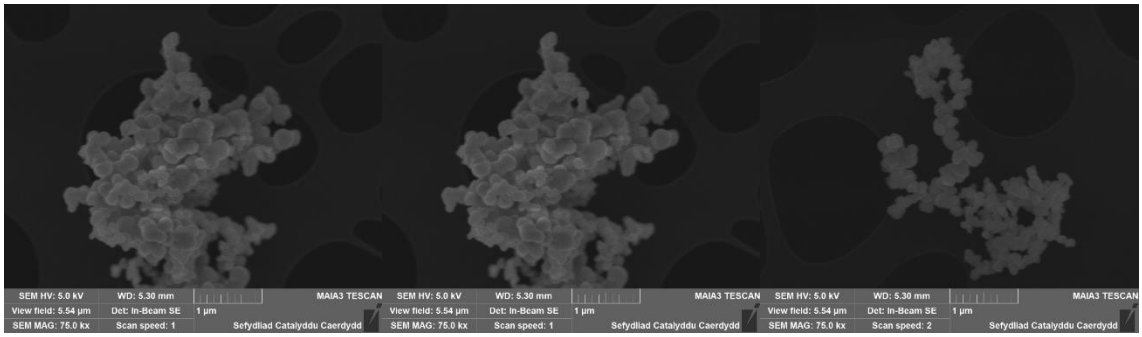

Fig S6. SEM images of FeMo_80P-7.5C-20W-5F.

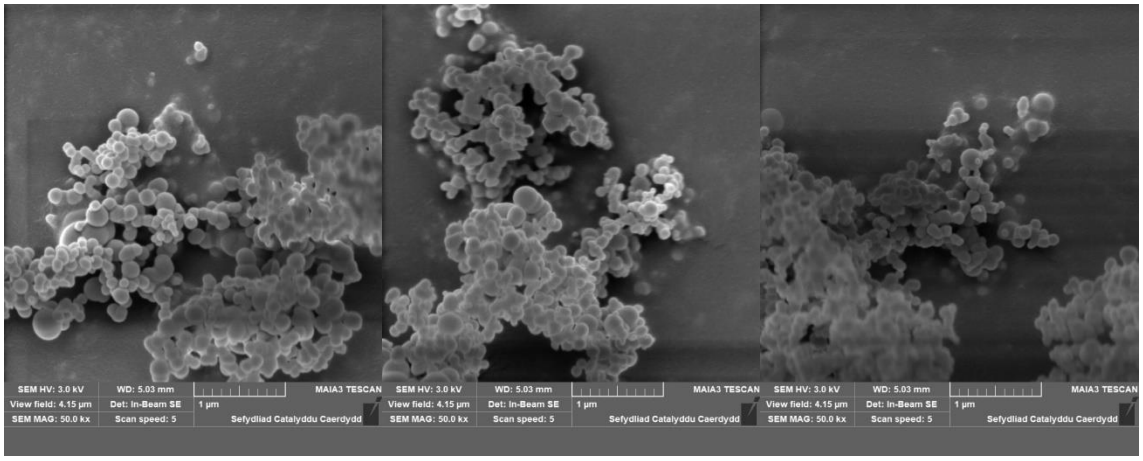

Fig S7. SEM images of FeMo_80P-10C-1W-5F

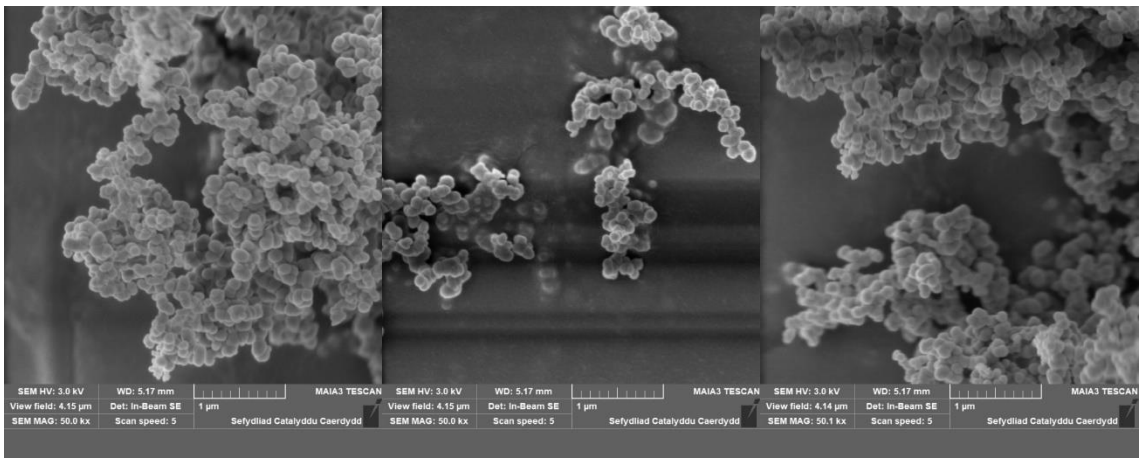

Fig S8. SEM images of FeMo_140P-5C-20W-10F.

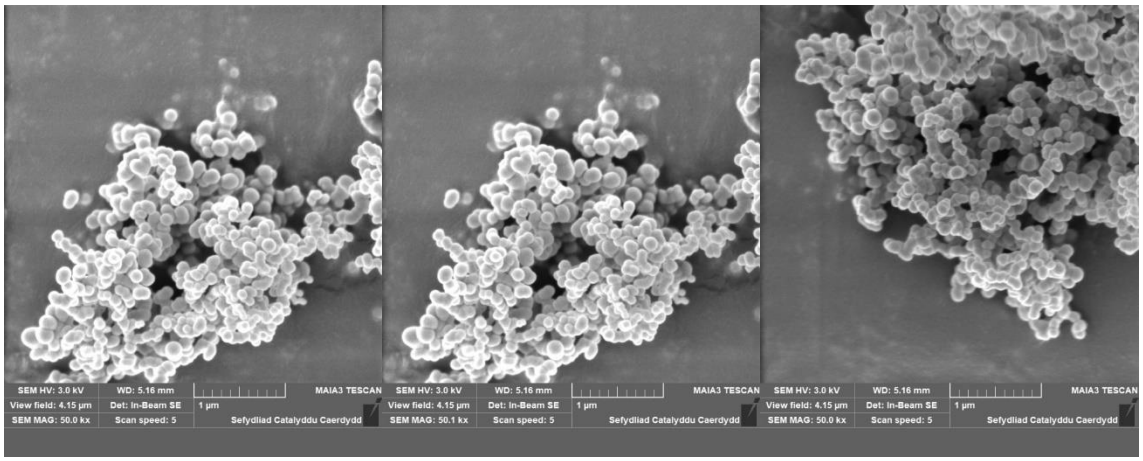

Fig S9. SEM images of FeMo_110P-7.5C-10.5W-7.5F.

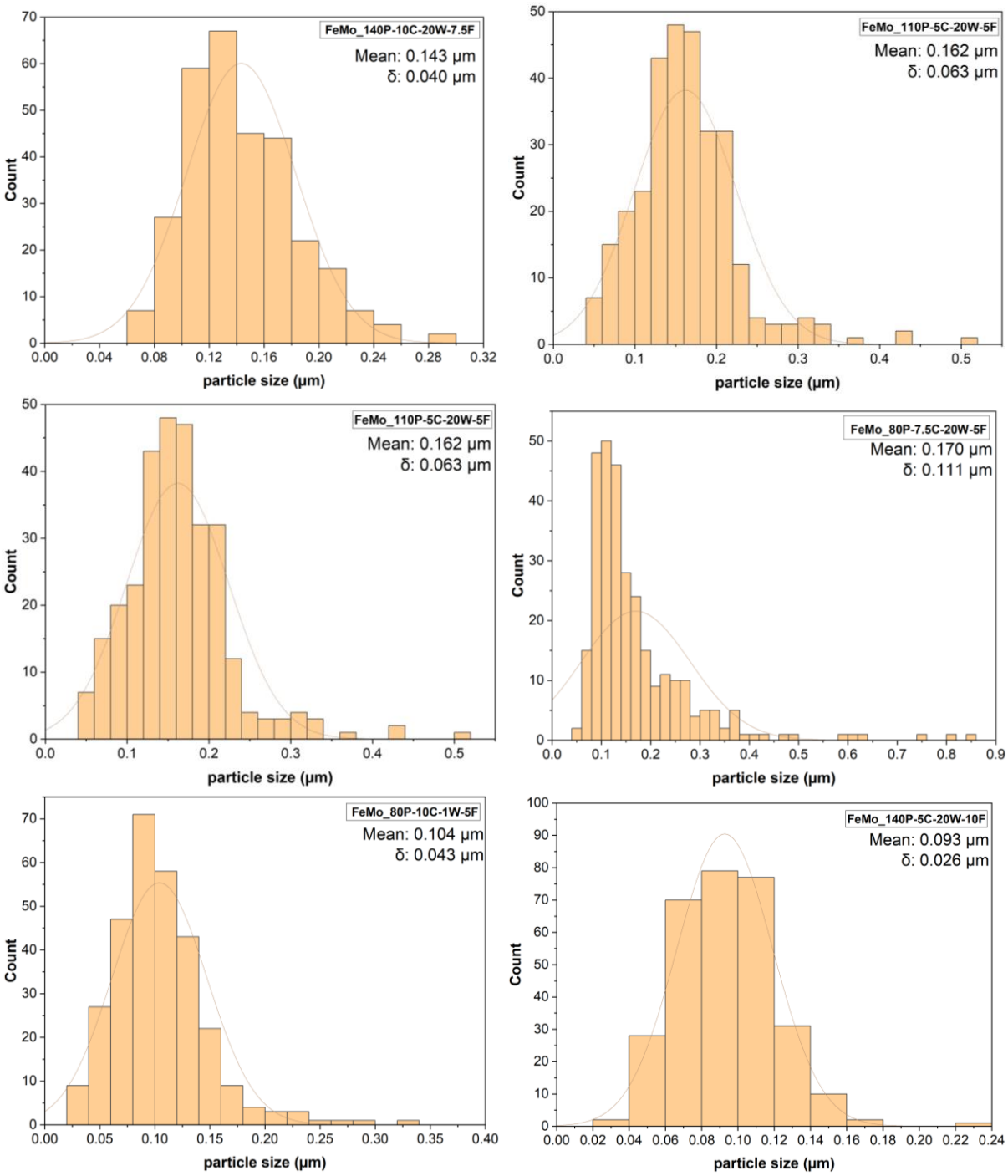
FeMo_140P-10C-20W-7.5F
Mean: 0.143 μm
δ: 0.040 μm
FeMo_110P-5C-20W-5F
Mean: 0.162 μm
δ: 0.063 μm
FeMo_110P-5C-20W-5F
Mean: 0.162 μm
δ: 0.063 μm
FeMo_80P-7.5C-20W-5F
Mean: 0.170 μm
δ: 0.111 μm
FeMo_80P-10C-1W-5F
Mean: 0.104 μm
δ: 0.043 μm
FeMo_140P-5C-20W-10F
Mean: 0.093 μm
δ: 0.026 μm
Count
particle size (μm)

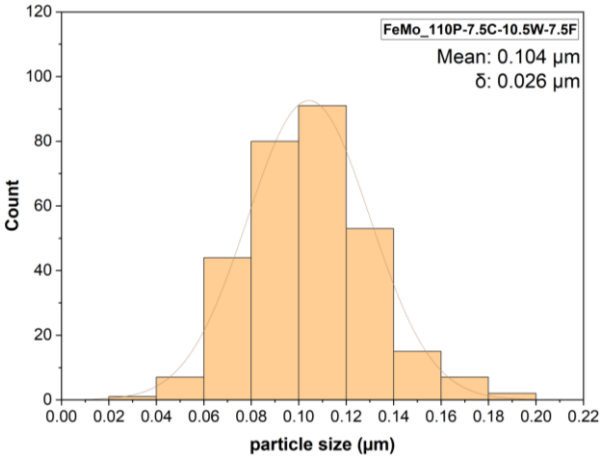

Fig S10. Particle size distribution of catalyst precursors.

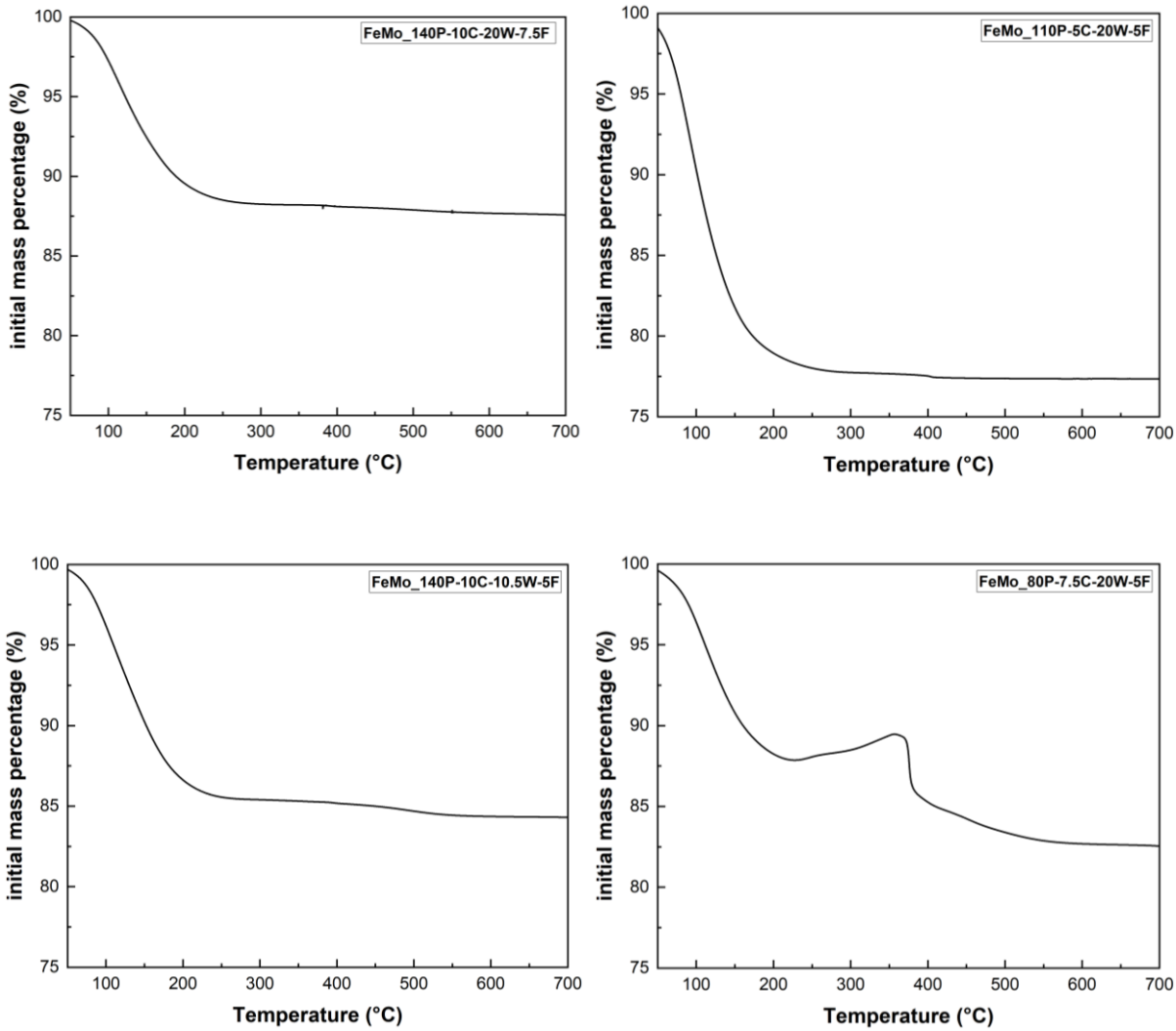

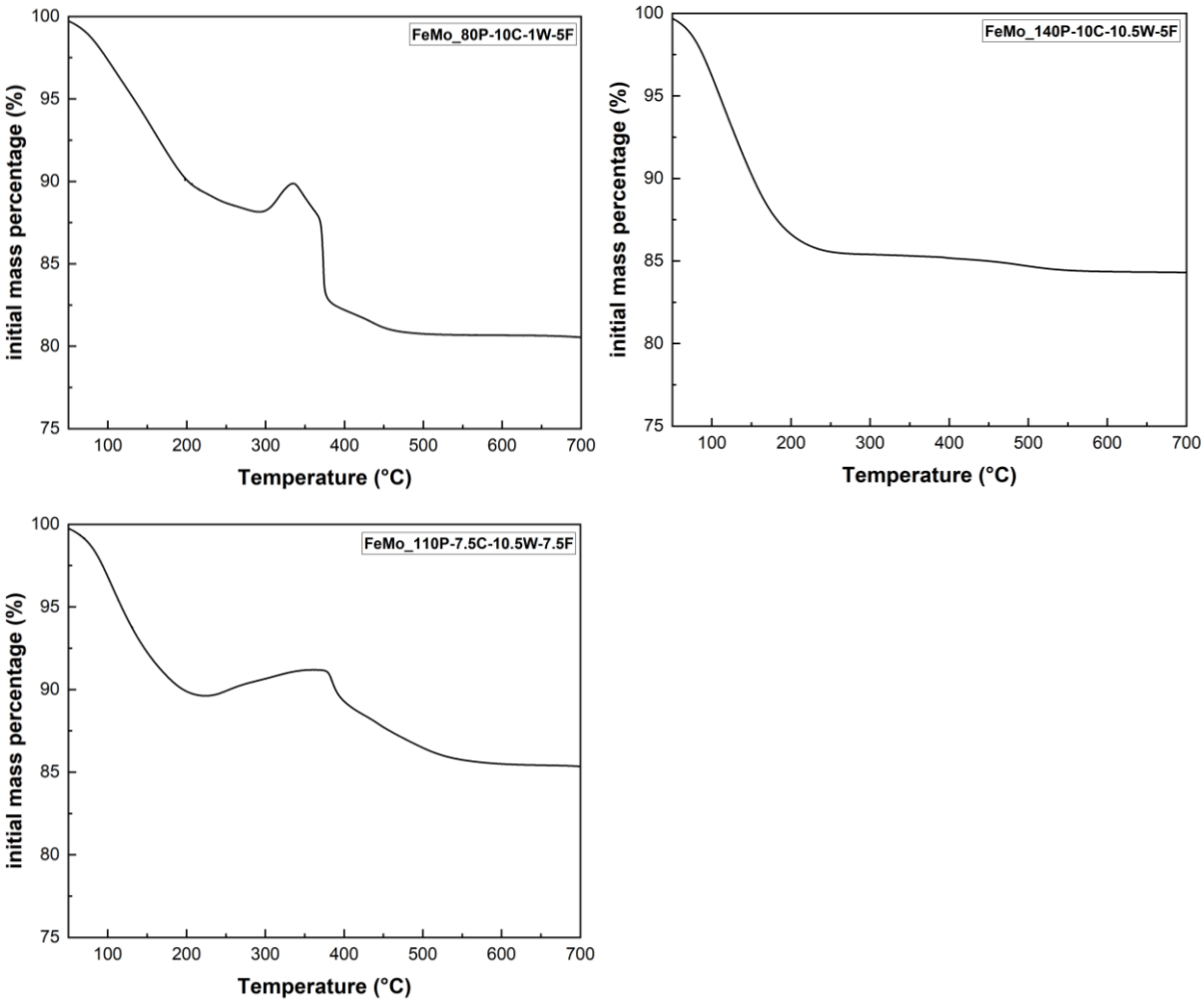

Fig S11. Thermogravimetric analysis of all catalyst samples formed by SAS precipitation.

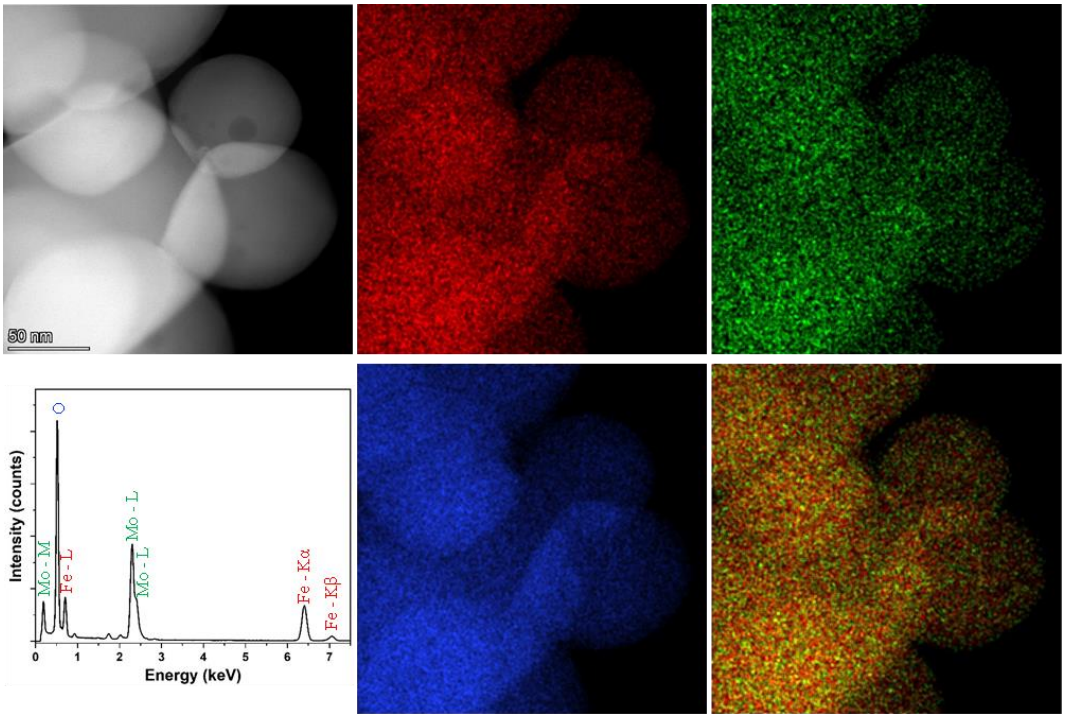

Fig S12. EDX Analysis of HAADF STEM images for FeMo_80P-10C-1W-5F.

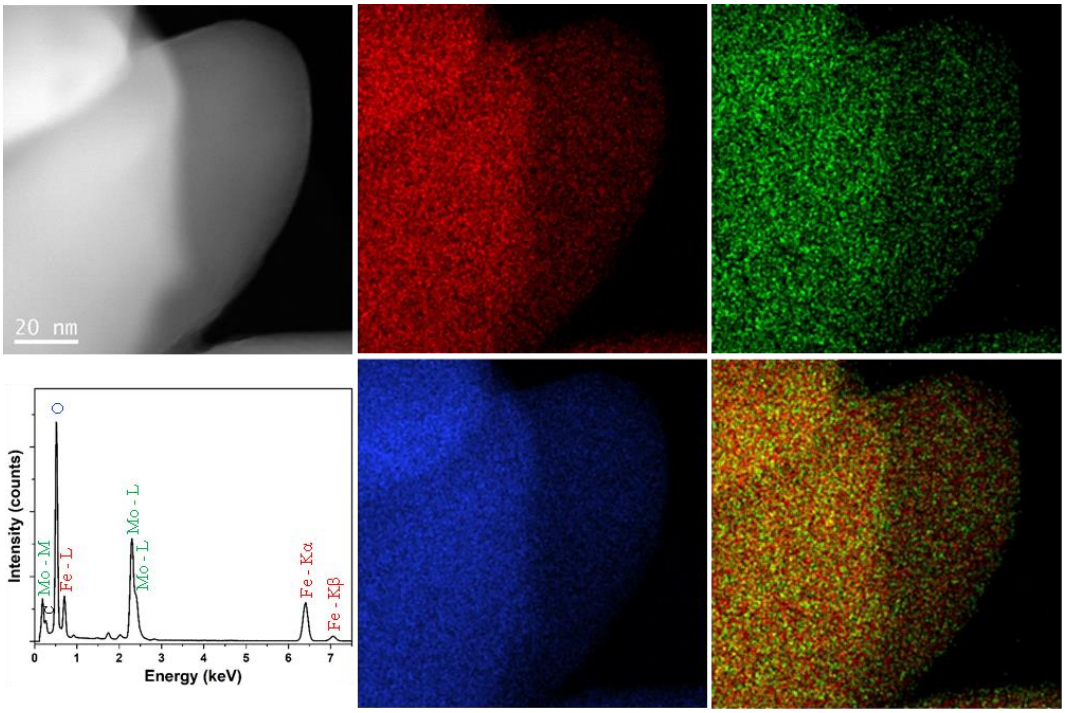

Fig S13. EDX Analysis of HAADF STEM images for FeMo_110P-5C-20W-7.5F.

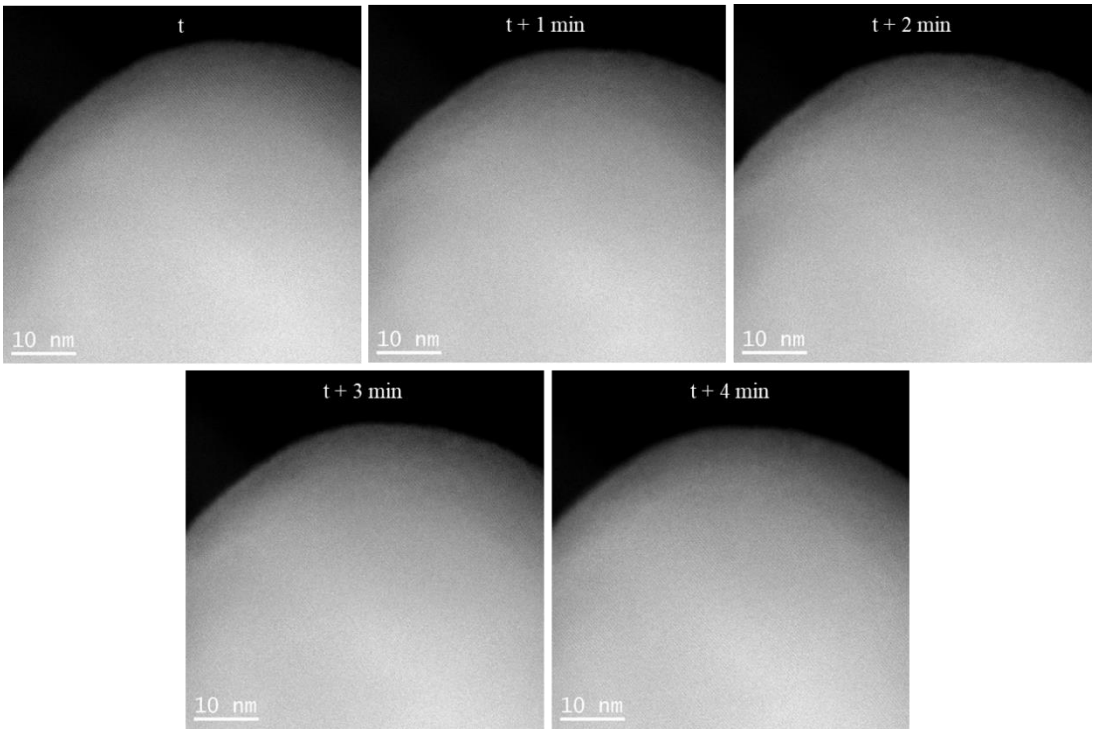

Fig S14. High resolution HAADF-STEM images of FeMo_80P-10C-1W-5F showing the effects of the electron beam on the amorphization of the structure. Electron dose is ~6600 $e^-/Å^2$ for each image.

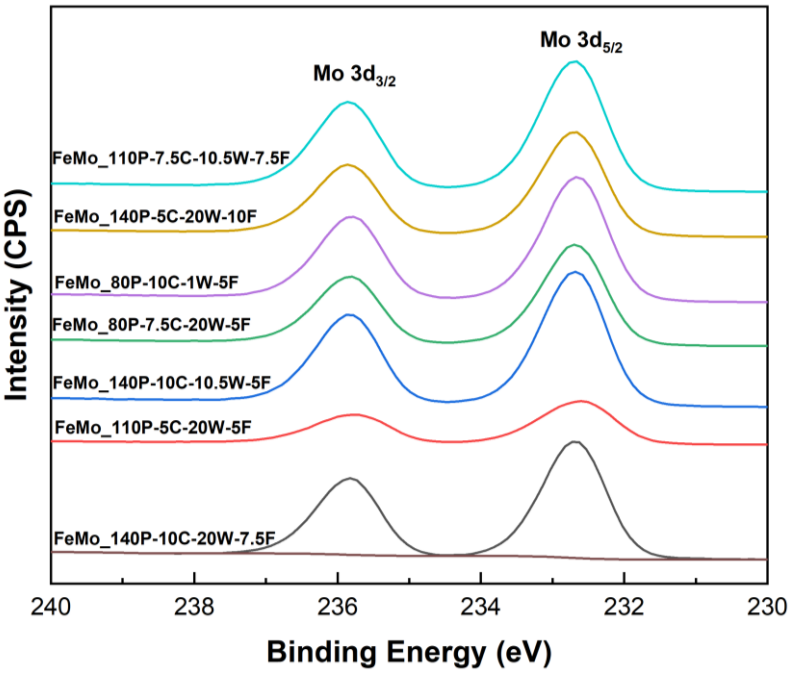

Fig S15. Mo 3d XPS spectra of novel iron molybdate catalysts formed.

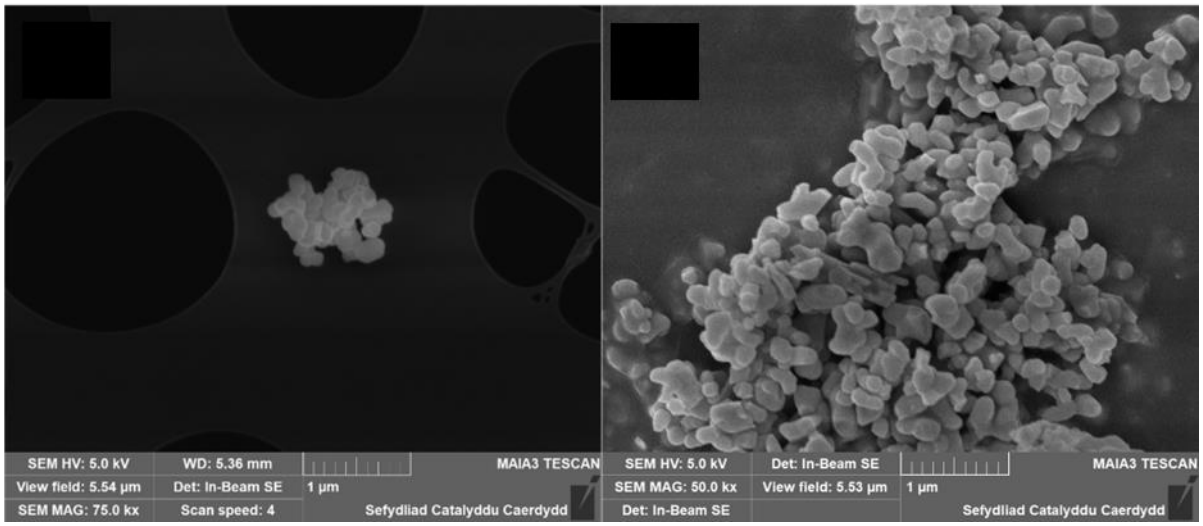

Fig S16. Comparison of precursor (left) and catalyst (right) morphology for FeMo_140P-10C-20W-7.5F.

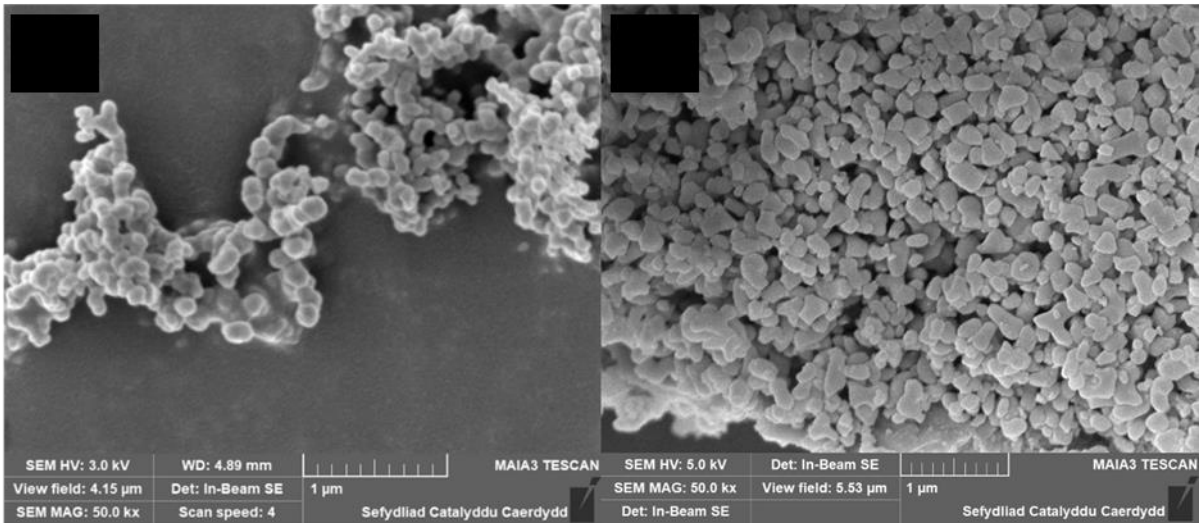

Fig S17. Comparison of precursor (left) and catalyst (right) morphology for FeMo_110P-5C-20W-5F.

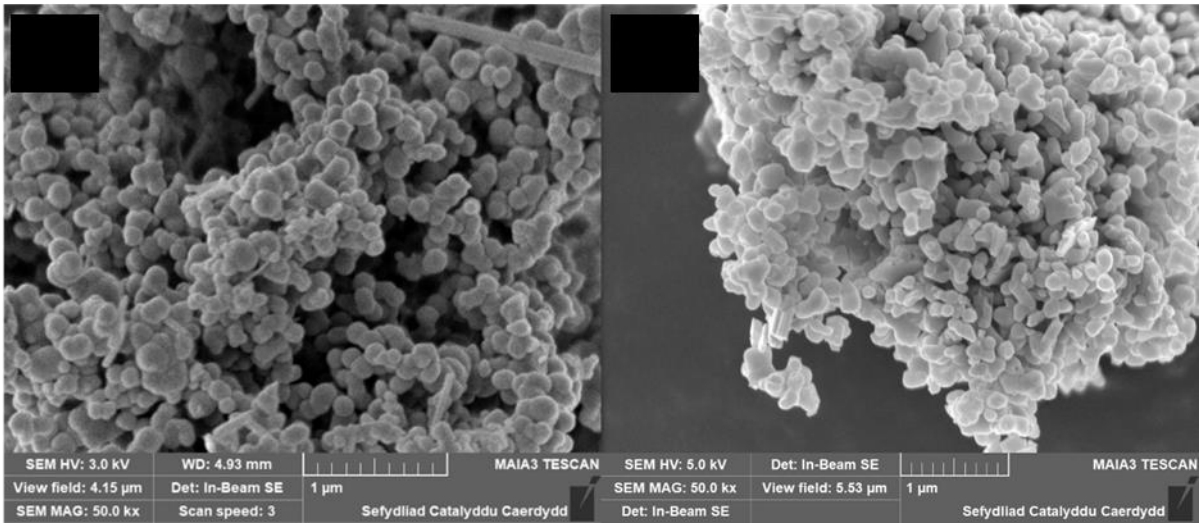

Fig S18. Comparison of precursor (left) and catalyst (right) morphology for FeMo_140P-10C-10.5W-5F.

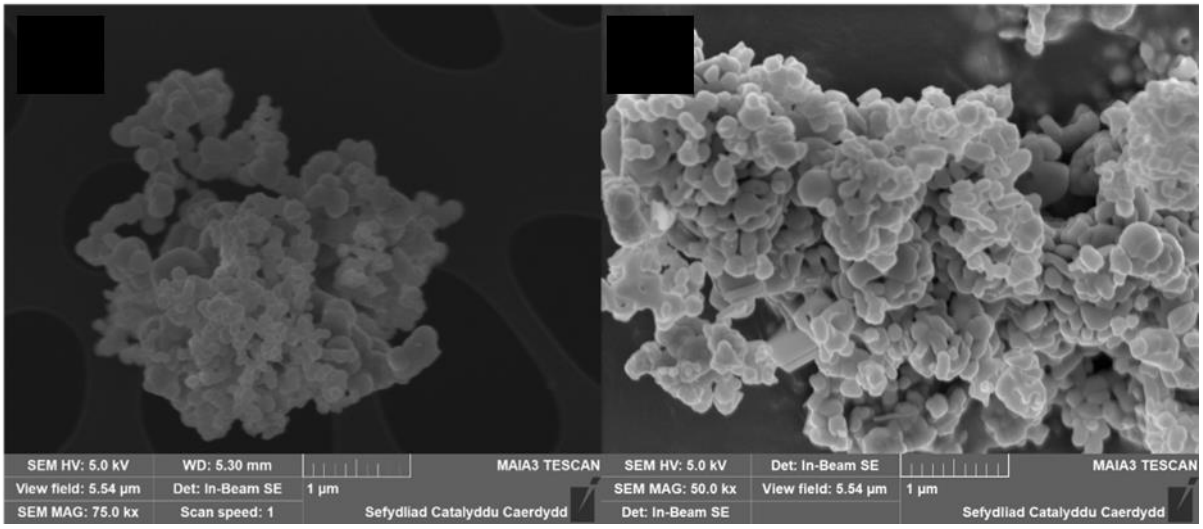

Fig S19. Comparison of precursor (left) and catalyst (right) morphology for FeMo_80P-7.5C-20W-5F.

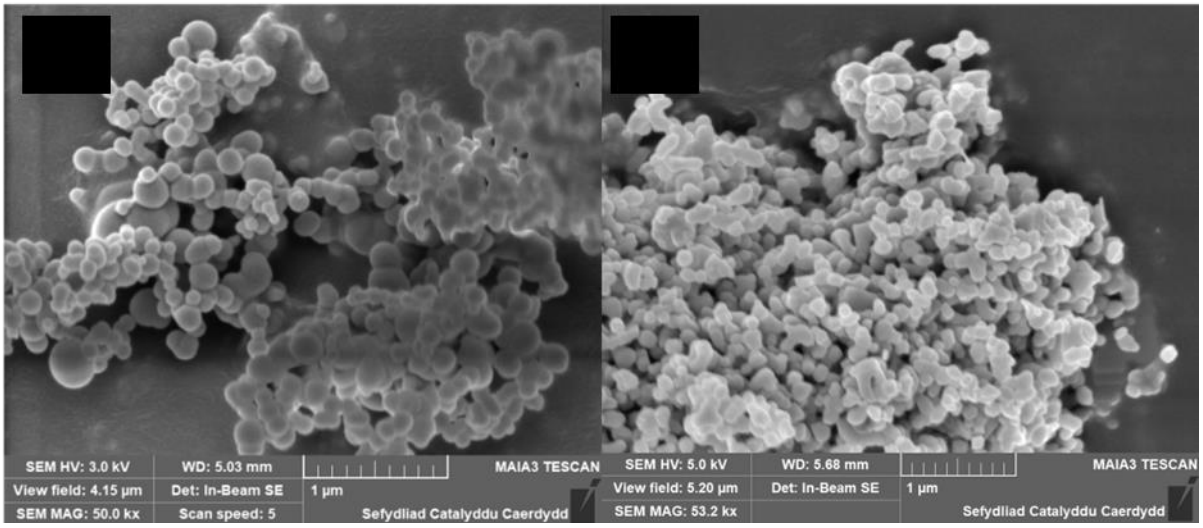

Fig S20. Comparison of precursor (left) and catalyst (right) morphology for FeMo_80P-10C-1W-5F

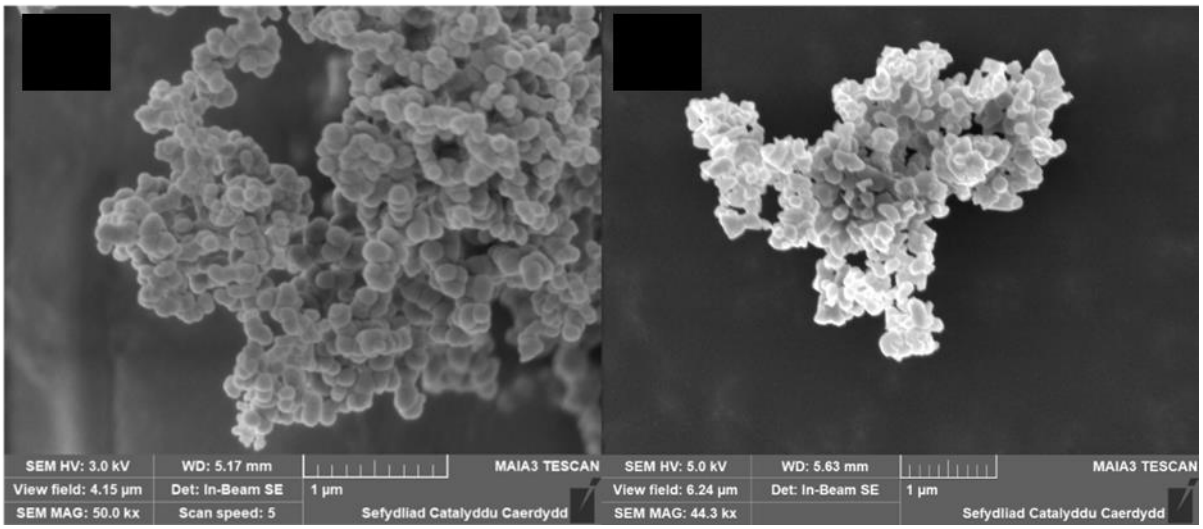

Fig S21. Comparison of precursor (left) and catalyst (right) morphology for FeMo_140P-5C-20W-10F.

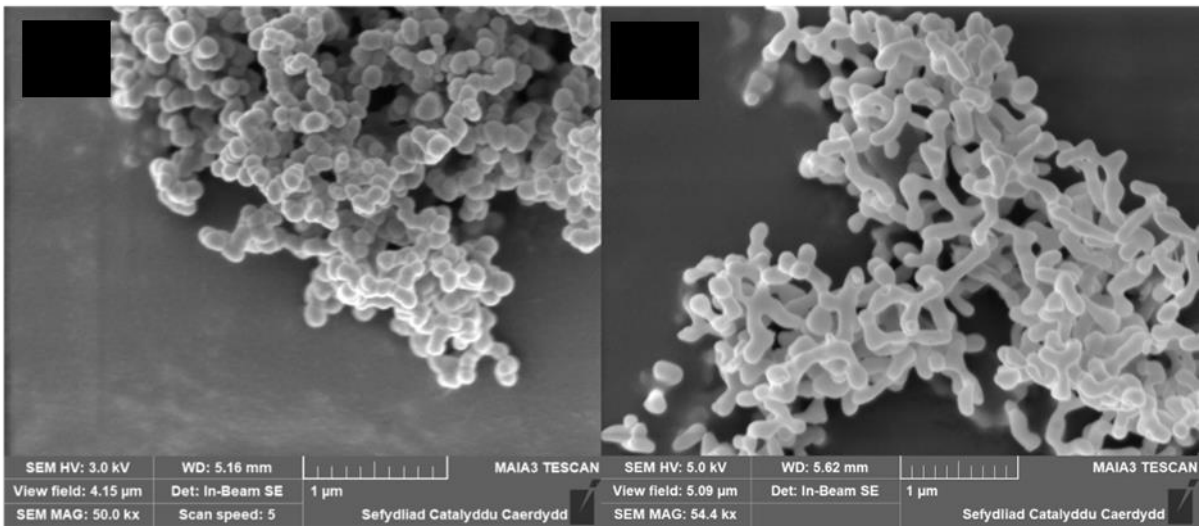

Fig S22. Comparison of precursor (left) and catalyst (right) morphology for FeMo_110P-7.5C-10.5W-7.5F.

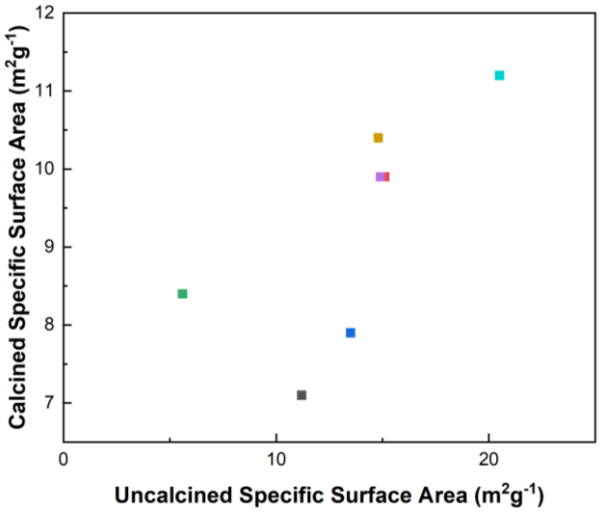

Fig S23. Relationship between uncalcined and calcined specific surface area.

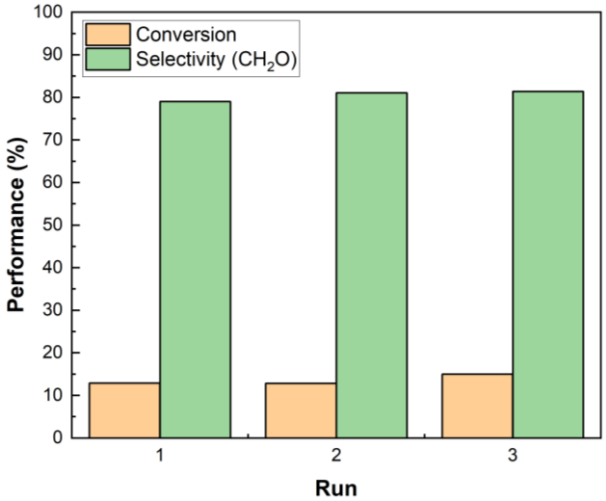

Fig S24. Repeat catalyst testing of FeMo_140P-5C-20W-10F for the selective methanol oxidation to formaldehyde. Isoconversion studies were conducted at 250 °C. The MeOH:O_2:N_2 ratio was 5:10:85 for all testing, with a total flow rate of 30 mL min^{-1}.

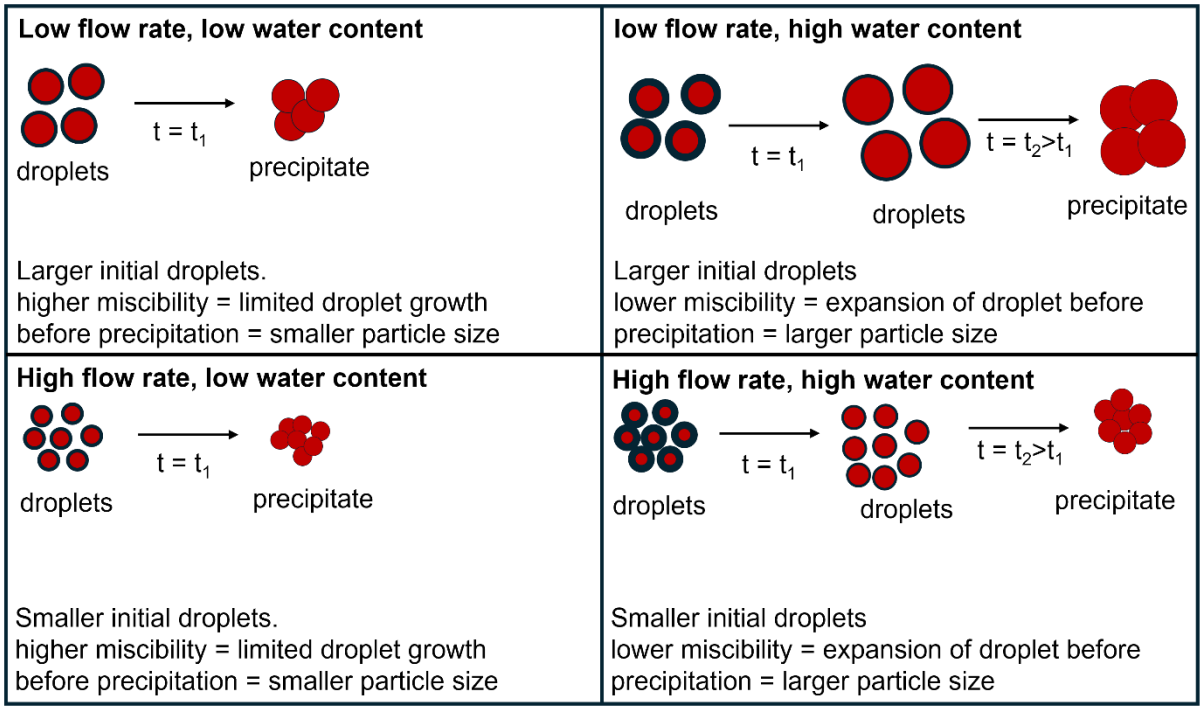

Fig S25: proposed relationships between particle size, solution flow rate and water content for SAS preparation.

Table S1. Comparison of productivity of catalysts formed in comparison to catalysts in literature.

Catalyst	Fe:Mo (1:x)	Temperature	WHSV	Productivity	Reference
		°C	g_{MeOH} g_{cat}^{-1} hr^{-1}	$mmol_{CH_2O}$ g_{cat}^{-1} hr^{-1}	
FeMo_140P-10C-20W-7.5F	1.58	250	7.4	25.4	This work
FeMo_110P-5C-20W-5F	1.37	250	10.7	42.5	This work
FeMo_140P-10C-10.5W-5F	1.66	250	7.9	33.7	This work
FeMo_80P-7.5C-20W-5F	1.55	250	8.4	26.6	This work
FeMo_80P-10C-1W-5F	1.61	250	6.7	25.6	This work
FeMo_140P-5C-20W-10F	1.50	250	9.8	33.3	This work
FeMo_110P-7.5C-10.5W-7.5F	1.60	250	9.4	36.6	This work
$FeMoO_x$ catalysts formed from metal oxalate precursor	1.5	260	0.785	18.6	[1]
$Fe_2(MoO_4)_3/MoO_3$ nanorods	1.6	260	0.785	12.8	[2]
$FeMoO_x$ catalysts formed from metal malonate precursor	1.5	260	0.785	6.35	[3]
Co-$FeMoO_x$ (Co:Mo = 0.05:1)	2.6	285	0.785	22.9	[4]
5 wt% MoO_3-CaHAP – MoO_3 supported on Ca doped hydroxyapatite		250	23.56	18.4	[5]
10 wt% MoO_3-CaHAP – MoO_3 supported on Ca doped hydroxyapatite		250	23.56	26.0	[5]

References

1 B. R. Yeo, G. J. F. Pudge, K. G. Bugler, A. V Rushby, S. Kondrat, J. Bartley, S. Golunski, S. H. Taylor, E. Gibson, P. P. Wells, C. Brookes, M. Bowker and G. J. Hutchings, *Surf Sci*, 2016, **648**, 163–169.

2 G. Jin, W. Weng, Z. Lin, N. F. Dummer, S. H. Taylor, C. J. Kiely, J. K. Bartley and G. J. Hutchings, *J Catal*, 2012, **296**, 55–64.

3 G. J. F. Pudge, G. J. Hutchings, S. A. Kondrat, K. Morrison, E. F. Perkins, A. V. Rushby and J. K. Bartley, *Catal Sci Technol*, 2022, **12**, 4552–4560.

4 X. Liu, L. Kong, S. Xu, C. Liu and F. Ma, *Front Chem Sci Eng*, 2021, **15**, 1099–1110.

5 J. Thrane, C. Falholt Elvebakken, M. Juelsholt, T. Lindahl Christiansen, K. M. Ø. Jensen, L. Pilsgaard Hansen, L. Fahl Lundegaard, U. Vie Mentzel, M. Thorhauge, A. Degn Jensen and M. Høj, *ChemCatChem*, 2021, **13**, 4954–4975.